SPE 113819

Finite Element Modelling of Casing in Gas Hydrate Bearing Sediments

Manoochehr Salehabadi, SPE, Min Jin, SPE, Jinhai Yang, Hooman Haghighi, SPE, Rehan Ahmed and Bahman Tohidi, SPE, Heriot-Watt University

This paper was prepared for presentation at the 2008 SPE Europec/EAGE Annual Conference and Exhibition held in Rome, Italy, 9–12 June 2008.

Abstract

Casing integrity in shallow marine sediments could be challenging if natural gas hydrates exist in the sediments. Elevated wellbore temperature during drilling of deeper sections of deep offshore wells can cause in-situ gas hydrates to dissociate, thereby increasing pore pressure and altering the mechanical properties of the sediments. Gas hydrate can also dissociate during setting and/or cementing, causing gas release which could result in delaying completion of the wellbore due to the flow of gas around the casing (conductor pipe) or affecting the casing integrity or casing stability by creating voids (channels) in the cement sheath leading to non-uniform stress loadings.

In this communication, a numerical model is developed using a finite-element code to simulate the stability of casing in gas hydrate bearing sediments by considering the interaction between the formation, the casing, and the cement with coupling the thermodynamic stability of the hydrates to hydraulic, mechanical and heat transfer terms. The mechanical and hydraulic terms are fully coupled and the coupling between mechanical and thermal terms is modelled through staggered technique (one-way coupling).

To model the worst-case scenario, the permeability of gas hydrate bearing sediments is assumed very low as a result the gas and water generated during gas hydrate dissociation cannot flow and will increase pore pressure. The mechanical property degradation of formation due to hydrate dissociation is represented in the model by cohesion softening as a function of dissociated gas hydrate saturation.

The developed numerical model is found to be very useful in understanding the behaviour of wellbores drilled in gas hydrate bearing sediments, which will help the determination of the resultant stress fields and enable a more accurate determination of the required casing strength.

Introduction:

Gas hydrates are ice-like crystalline compounds formed from mixtures of water and suitably sized 'guest' molecules and stable under low temperature and high-pressure conditions. Guest molecules in natural hydrates are either methane or a mixture of components comprising natural gas. Typically, they are found in sediments within a few hundred meters of the seafloor, in water depths of around 500m depending on seabed temperature, gas composition, and geothermal temperature gradient. An increase in the system temperature and/or a reduction in the system pressure could result in gas hydrates dissociation, and production of water and gas. As gas hydrates store large quantities of gas (around 172 vol/vol), their dissociation will result in the release of large amounts of gas.

The presence of gas hydrate is one of the problems when developing conventional oil and gas fields in deepwater offshore. To-date gas hydrate bearing sediments have been drilled through without any major problems in numerous locations in the Canadian and Alaskan arctic, and Gulf of Mexico (Tan, et al, 2005), (Smith, et al, 2005). The techniques used to overcome drilling problems are reducing the drilling fluid temperature, increasing the hydrostatic mud pressure and chemically stabilizing the gas hydrate (Tan, et al, 2005). Nevertheless the lack of a tool to predict the behaviour of the well drilled in gas hydrate bearing sediments, has resulted in a strategy of avoiding hydrate bearing sediments when locating deep offshore production platforms. This could increase the cost of development for deep offshore oil and gas fields.

Casing stability is an important part of the well design, therefore it is necessary to develop a tool to predict casing behaviour for wells drilled in gas hydrate bearing sediments. Standard casing design ignores the interaction of casing-cement-formation on the required strength of casing (Berger, et al, 2004). Indeed, there is not a simple method available to determine the magnitude of this effect. In addition, the conventional casing design fails to account for the non-uniform loaded casing.

However, Berger, et al. (2004) and Fleckenstein, et al. (2005) developed a model in ANSYS code to study the effect of non-uniform loading on casing stability for wells drilled in formations containing hydrocarbons (but not gas hydrates).

There are different sources that can cause non-uniform loading on the casing during drilling. Voids or channels in the cement sheath behind the casing is one of the non-uniform loading sources which is likely to happen in the wells drilled in gas hydrate bearing sediments due to partial dissociation (melting) of hydrates and gas release during setting or cementing of the casing. The non-uniform loading could also happen when the drilling of next section of the wellbore after running and cementing the casing in gas hydrate-bearing sediments. The deeper sections below the GHSZ (Gas Hydrate Stability Zone) is hotter than the above, so heat transfer between the drilling mud in the casing and around a wellbore during drilling the deeper sections could dissociate gas hydrates and cause overpressures behind the casing in low permeability gas hydrate formation. Pore pressure increase in the formation combined with potential void (channel) in the cement sheath behind the casing is a source of non-uniform loading on the casing during drilling in gas hydrate bearing sediments.

Most of the investigations conducted so far, were about characterization of hydrates in sediments and gas production from gas hydrate reservoirs. Potential wellbore failures remain uncertain because there are no simple tools to quantify them. Yousif, et al. (1990, 1991) studied hydrate dissociation in Berea sandstone using Kim-Bishnoi kinetic model (Kim, et al, 1987) by depressurization. Moridis (2002) developed TOUGH2 reservoir simulator to consider hydrate dissociation using both equilibrium and kinetic reaction. Ahmadi, et al. (2007) modelled gas production from gas hydrate reservoirs using an axisymmetric model. The developed gas hydrate reservoir simulators are mainly focused on production of methane from gas hydrate reservoirs and they consider gas hydrate bearing sediments as a rigid body in their calculations. It means that they assumed that gas hydrate is found in such formations that do not deform; however, some of these models consider pore volume compressibility (Swinkels, et al, 2000) in the calculations. Recently Birchwood, et al. (2005) developed a semi-analytical wellbore stability model using mechanical properties of THF (TetraHydroFuran) hydrate without taking into consideration casing stability. Klar, et al. (2005) developed a geomechanical model in FLAC 2D code to study the wellbore stability during gas production from gas hydrate reservoirs by isothermal depressurization. Two-phase flow (water and gas) equations, assuming gas hydrate as a non-flowing phase, were used to model two phase flow of liquid and gas during gas hydrate dissociation. Kim-Bishnoi kinetic reaction equation is used to model gas hydrate dissociation during depressurization. Nevertheless, they did not consider heat transfer in their model. Rutqvist, et al. (2007) coupled TOUGH-FX/HYDRATE as a numerical simulator of hydrate reservoir with FLAC 3D as a commercial geomechanical code to develop a numerical code considering the three essential terms (i.e., hydraulic, mechanical and thermal) for analysing the stability of gas hydrate bearing sediments under mechanical and thermal stresses. However, in their modelling, they considered wellbore assembly as a rigid and fixed boundary condition; in fact, they investigated the effect of the geomechanical modelling on the previous studies that had done by Moridis, et al. (2006). Kimoto, et al. (2007) developed a chemo-thermo-mechanical finite element model to study the geomechanical effects of hydrate dissociation during thermal stimulation or depressurization. In their model Darcy's law is used to simulate gas and water (generated during hydrate dissociation) flow in porous media. An elasto-viscoplastic constitutive model adapted for modelling soil behaviour with considering the effect of hydrate. Kim-Bishnoi kinetic reaction equation is used to model gas hydrate dissociation. Again, in this model the simulation is not taking into consideration the stability of casing. Freij-Ayoub, et al. (2007b) developed a model in FLAC 3D finite difference code to study the stability of wellbore supported with casing in gas hydrate bearing sediments under uniform loading during gas hydrate dissociation and did not consider non-uniform loading. Their model assumes that the mechanical behaviour of sediments follow Mohr-Coulomb constitutive model with decreasing cohesion corresponding to hydrate saturation decreasing in the pore space during dissociation. Hydrate dissociation is modelled under thermal stimulation with a simple algorithm. The model considers interaction between cement and casing by defining interaction bond properties between cement and casing. Fluid generated during hydrate dissociation is considered a single phase with Darcy law for fluid flow in the porous media.

In this study, we look into casing stability of wellbores drilled in gas hydrate bearing sediments under uniform and non-uniform loading. Non-uniform loading is introduced in the system by considering voids in the cement sheath behind the casing together with the pore pressure increasing due to gas hydrate dissociation as a result of hot mud circulation inside the casing during drilling of deeper sections of the well. This study is new in the considered scenarios because it investigates the effect of both uniform and non-uniform loading on the casing stability in gas hydrate bearing sediments and it is the first time that ABAQUS is used for this kind of modelling. ABAQUS is used for this study as it has thermal, hydraulic and mechanical analysis in porous medium that are three necessary terms in geomechanical modelling of gas hydrate bearing sediments, in addition ABAQUS has other special capabilities which can be used to model different scenarios in geomechancial modelling of gas hydrate bearing sediments in the future.

Numerical Modelling:

The model is developed to simulate the casing stability for wells drilled in gas hydrate bearing sediments. The in-situ stresses are assumed isotropic (Birchwood, et al, 2005) and the effect of drilling fluid inside the casing (i.e., internal pressure) on the mechanical strength of the casing has been taken into account (in addition to collapse strength of casing). The casing, cement and formation elements are plane strain, eight node continuum elements. The formation elements contain an additional degree of freedom to accommodate pore pressure. When the formation is heated, the gas hydrate behind the cement sheath will dissociate and result in an increase in the formation pore pressure. HWHYD, the

Heriot-Watt Hydrate model (Tohidi, et al, 1995), is used and implemented into the code to model the hydrate stability zone and quantifying the pore pressure increase due to hydrate dissociation by thermal stimulation. In the developed model, we assumed that there is a good bond between cement and casing but we assumed that there is a contact interaction between the cement and formation containing gas hydrates. It is assumed that heat transfer takes place by conduction only and the formation permeability is low enough that water and gas generated during gas hydrate dissociation cannot flow out. The heat transfer term is coupled to hydraulic and mechanical deformation terms through staggered method (one-way coupling). All material properties used in the modelling were obtained from available literatures (Callister, 2007), (Birchwood, et al, 2005), (Freij-Ayoub, et al, 2007a, b), (Fleckenstein, et al, 2000), (Moridis, et al, 2006).

Governing Equations:

The description and mathematical equations of each term (mechanism) considered in this study are presented below, more details of these equations could be found elsewhere (ABAQUS User`s Manual):

Hydraulic- Mechanical Analysis

The hydraulic and mechanical deformation terms are fully coupled in the ABAQUS. The coupling is based on the equilibrium, constitutive and mass conservation equations using the effective stress theory.

Equilibrium:

Equilibrium is expressed by writing the principle of virtual work for the volume under consideration in its current configuration:

$$\int_V \sigma : \delta\varepsilon \, dV = \int_S t.\delta v dS + \int_V f.\delta v dV \quad \text{..... (1)}$$

where δv is a virtual velocity field, $\delta\varepsilon$ is the virtual rate of deformation, t are surface tractions per unit area, and f are body forces per unit volume.

The effective stress equation is:

$$\overline{\sigma} = \sigma + U_w I \quad \text{..... (2)}$$

where I is the unitary matrix. In ABAQUS, stress components are stored so that the tensile stress is positive.

Constitutive equations

The constitutive equation for the solid is expressed as:

$$d\sigma = H : d\varepsilon + a \quad \text{..... (3)}$$

where H is the material stiffness and a is any strain independent contribution (thermal expansion)

Mass Conservation

A continuity equation is used to relate the rate of increase in the liquid mass stored at a point to the rate of mass of liquid flowing into the point within the time increment:

$$\frac{d}{dt}\left(\int_V \rho_w n dV\right) = -\int_S \rho_w n V_w dS \quad \text{..... (4)}$$

The liquid flow is described by introducing Darcy's law:

$$S_r n V_w = -\hat{K}.\frac{\partial \phi}{\partial X} \quad \text{..... (5)}$$

Uncoupled heat transfer

Energy balance

The basic energy balance is:

$$\frac{d}{dt}\int_V \rho U dV = \int_S q dS + \int_V r dV \quad \text{..... (6)}$$

where U is the internal energy; q is the heat flux per unit area of the body, flowing into the body; and r is the heat supplied externally into the body per unit volume.
It is assumed that the thermal, hydraulic and mechanical terms are weakly coupled (one-way coupling) such that porous medium deformation and pore fluid flow do not affect on heat transfer and temperature distribution.

Constitutive definition

$$c_h = \frac{dU}{dT} \quad \text{..... (7)}$$

Heat conduction is assumed to be governed by the Fourier law:

$$f_f = -k_c \frac{\partial T}{\partial x} \quad \text{..... (8)}$$

f_f is the heat flux; and x is position.

Thermal-Hydraulic-Mechanical Coupling:

ABAQUS does not have element with fully THM (Thermal-Hydraulic-Mechanical) coupling, which means that Jacobian matrix for hydraulic-mechanical equations and thermal equations is derived separately (Rutqvista, et al, 2001). The method is used to couple thermal and hydraulic-mechanical analysis is the staggered solution technique. It is assumed that pore fluid flow and displacements do not affect the temperature distribution (one-way coupling). Figure 1 shows the computational process, which is used in this study. First, the temperature distribution generated from thermal analysis is written to an external file then the hydraulic-mechanical model coupled with thermodynamic model reads an external file and calculates the stress, pore pressure and displacement, etc generated due to gas hydrate dissociation.

Thermodynamic Model:

Hydrate could dissociate due an increase in the system temperature and/or a decrease in pressure to outside the hydrate stability zone. Gas hydrate dissociation produces water and gas, resulting in excess pore pressure due to the volume expansion associated with the dissociation. There are two approaches for predicting hydrate dissociation. The first approach considers hydrate dissociation at equilibrium while the second one considers it as a kinetic reaction. The modelling results of the gas hydrate production from gas hydrate reservoirs using both approaches are in many cases remarkably similar (Kowalsky, et al, 2007). In this study, gas hydrate dissociation is assumed to occur close to thermodynamic equilibrium and the HWHYD model is used to quantify the pore pressure increase due to hydrate dissociation. In this model, the well-proven Valderrama modification of the Patel-Teja (VPT) equation of state combined with non-density-dependent mixing rules is used to model the fluid phases. Hydrates are modelled using the solid solution theory of van der Waals and Platteeuw. More information on the thermodynamic modelling could be found elsewhere (Tohidi et al, 1995)

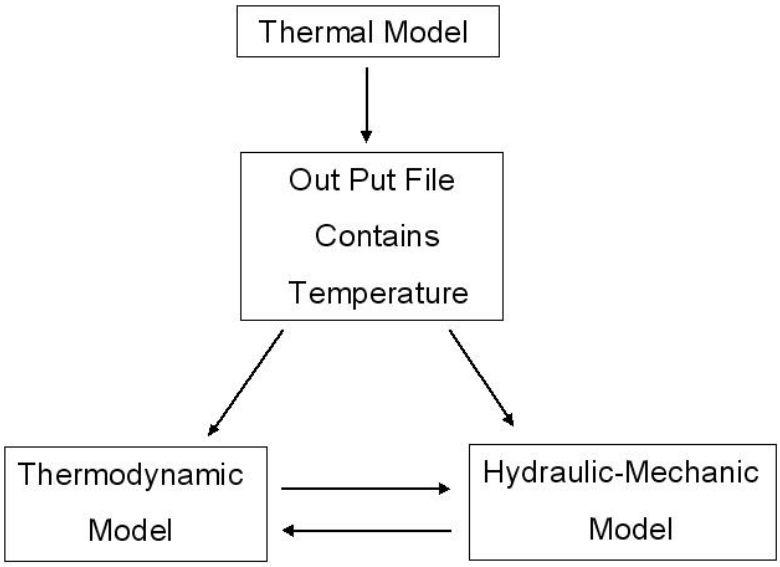

Figure1-Diagram of the computational process

Hydrate Saturation Calculations during dissociation:

The strength of sediments containing gas hydrates depends on the hydrate saturation (Kimoto, et al, 2007). Gas hydrates have a bonding effect on sediment particles. Furthermore, they are part of load bearing component of the sediment (Helgerud, et al, 2000). It is assumed in this study that cohesion softening of the sediments during gas hydrate dissociation is a function

of the reduction in gas hydrate saturation in the sediments during dissociation as represented by Equation 9 (Freij-Ayoub, et al, 2007a).

$$C = C_0 * (1 - 1.2 * (dS_h)) \ldots\ldots\ldots\ldots (9)$$

All calculations of the cohesion softening associated with decreasing hydrate saturation during dissociation are performed according to the method described by Xu (2006).

Suppose that a mixture of liquid water, free gas and gas hydrate resides in pore volume, V_p the volume of gas hydrates is:

$$V_h = V_p * S_h \ldots\ldots\ldots\ldots (10)$$

where S_h is the volume fraction of gas hydrate averaged over V_p. The total volume change dV resulting from the dissociation of a small dV_h gas hydrates, which releases dV_w water and dV_g free gas, includes the volume change due to the fact that the densities of released water and free gas are different from that of the dissociating gas hydrate and the volume change due to the compressibility of extant free gas, liquid and gas hydrate.
The first volume change $(dV)_1$, related to density differences is:

$$(dV)_1 = dV_w + dV_g + dV_h \ldots\ldots\ldots\ldots (11)$$

The amount of gas dissolved in the released water is small, in comparison with the gas released due to hydrate dissociation. Therefore, the contribution of the dissolved gas to the volume change is usually negligible. As a result, for a fixed gas mass fraction r_g of the gas hydrate:

$$dV_g = \frac{dM_g}{\rho_g} = -r_g * \frac{dM_h}{\rho_g} = -r_g * (\frac{\rho_h}{\rho_g}) * dV_h \ldots\ldots\ldots\ldots (12)$$

$$dV_w = \frac{dM_w}{\rho_w} = -(1 - r_g) * \frac{dM_h}{\rho_w} = -(1 - r_g) * (\frac{\rho_h}{\rho_w}) * dV_h \ldots\ldots\ldots\ldots (13)$$

where ρ_w, ρ_g, ρ_h and M_w, M_g, M_h denote the densities and the masses of the liquid water, the free gas and the gas hydrate, respectively. Thus the volume change relative to constant pore volume V_p is:

$$\frac{(dV)_1}{V_p} = -R_v * \frac{dM_h}{V_p} = -R_v * dS_h \ldots\ldots\ldots\ldots (14)$$

where

$$R_v = (1 - r_g) * \frac{\rho_h}{\rho_w} + r_g * \frac{\rho_h}{\rho_g} - 1 \ldots\ldots\ldots\ldots (15)$$

R_v Is the factor of volume expansion resulting from gas hydrate dissociation. Variations of ρ_w, ρ_h and r_g are usually negligible.

The second part of the total volume change is related to the compressibility of existing free gas, gas hydrate and liquid solution. Assuming thermodynamic equilibrium, the effective compressibility, K of the mixture of free gas, gas hydrate and liquid solution along the gas hydrate stability may be calculated as:

$$K = -\frac{1}{V}\left(\frac{\partial V}{\partial P} + \frac{\partial V}{\partial T} * \frac{dT_e}{dP}\right) = \frac{S_g}{\rho_g} * \left(\frac{\partial \rho_g}{\partial P} + \frac{\partial \rho_g}{\partial T} * \frac{dT_e}{dP}\right) + \frac{S_w}{\rho_w} * \left(\frac{\partial \rho_w}{\partial P} + \frac{\partial \rho_w}{\partial T} * \frac{dT_e}{dP}\right) + \frac{S_h}{\rho_h} * \left(\frac{\partial \rho_h}{\partial P} + \frac{\partial \rho_h}{\partial T} * \frac{dT_e}{dP}\right) \quad \ldots\ldots\ldots\ldots (16)$$

where T_e is the stability temperature of gas hydrate at the given pressure, and S_g, S_h and S_w are the pore space volume fractions of free gas, gas hydrate and liquid solution, respectively. When there is no pressure change other than the excess pore pressure (P_{ex}) resulting from gas hydrate dissociation, the relevant volume change is:

$$\frac{(dV)_2}{V_p} = -K * dP_{ex} \ldots\ldots\ldots\ldots (17)$$

Since the sediment permeability is assumed sufficiently low, the dissociation process is treated as taking place in a constant pore volume so the total volume change is zero and we can calculate the hydrate saturation changes (dS_h) during dissociation from the following equation:

$$\frac{dV}{V_p} = \frac{(dV)_1}{V_p} + \frac{(dV)_2}{V_p} = (-R_v * dS_h) - (K * dP_{ex}) = 0 \ldots\ldots\ldots\ldots (18)$$

Material Properties:

The material properties used in this study are summarized as following and presented in Table 1

Table 1-Material properties

Casing Properties		**Cement Properties**	
Thickness (m)	0.025 or 1 in	Thickness (m)	0.05 or 2 in
Yield Stress (MPa)	375	Density (kgm^{-3})	2200
Weight (kgm^{-1})	494	Young's Modulus , System #1, (MPa)	4758.501
Young's Modulus (MPa)	210000	Poisson Ratio, System #1	0.42
Poisson Ratio	0.3	Compressive Strength, System #1, (MPa)	6.896
Density (kgm^{-3})	2200	Tensile Strength, System #1, (MPa)	0.207
Thermal Expansion (K^{-1})	0.0000037	Weight (ppg) , System #1	12.1
Thermal Conductivity ($Wm^{-1}K^{-1}$)	15	Young's Modulus, System #2, (MPa)	5517.103
Heat Capacity ($JK^{-1}kg^{-1}$)	450	Poisson Ratio, System #2	0.32
Formation Properties		Compressive Strength, System #2, (MPa)	17.241
Young's Modulus (Mpa)	807.6	Tensile Strength, System #2, (MPa)	1.379
Poisson Ratio	0.40	Weight (ppg) , System #2	13.8
Density (kgm^{-3})	2200	Thermal Expansion (K^{-1})	0.000015
Porosity	49 %	Thermal Conductivity, System A, ($Wm^{-1}K^{-1}$)	2.4
In-situ Temperature (K)	288	Thermal Conductivity, System B, ($Wm^{-1}K^{-1}$)	0.66
In-situ Pore Pressure (MPa)	18	Heat Capacity, System A , ($JK^{-1}kg^{-1}$)	835
In-situ Stress (MPa)	24	Heat Capacity, System B , ($JK^{-1}kg^{-1}$)	2100
Cohesion (MPa)	3.2	**Pore Fluid Properties**	
Friction Angel (^{o})	30	Density (kgm^{-3})	1000
Thermal Expansion (K^{-1})	0.000077	Thermal Expansion (K^{-1})	0.0003
Thermal Conductivity ($Wm^{-1}K^{-1}$)	1.4	Thermal Conductivity ($Wm^{-1}K^{-1}$)	0.6
Heat Capacity ($JK^{-1}kg^{-1}$)	1900	Heat Capacity ($JK^{-1}kg^{-1}$)	4181.3
In-situ Hydrate Saturation	20 %	Mud Weight (ppg)	8.5

Formation:

The formation is assumed to have porosity of 49 percent and is modelled as perfect plastic Mohr-Coulomb with cohesion softening (Freij-Ayoub, et al, 2007a), (Birchwood, et al, 2005).

Casing:

The casing is modelled as elastic/perfectly plastic material.

Cement:

When the principal stress components are dominantly compressive, the response of the cement is modelled by an elastic-plastic theory using a simple form of yield surface. Associated flow and isotropic hardening are used and when the principal stress components are tensile, the response of the cement is modelled by cracking. Cracking is assumed to occur when the stress reaches a cracking failure surface. When a crack has been detected, its orientation is stored for subsequent calculations and it is irrecoverable, it remains for the rest of the calculation but may open and close following crack detection, the crack affects the calculations because a damaged elasticity model is used. For investigating the effect of cement with different mechanical properties on the casing stability, the mechanical properties of two different system of cement designed for shallow depths were used in the modelling.

System 1 contained a cement/siliceous material mixture, 30% latex by weight of water (BWOW), mixed at 12.1 ppg with 10.81 gallons mix water per sack of cement (Fleckenstein, et al, 2000).

System 2 contained a cement/pozzolan mixture, 10 lbs/sack silica flour, 30% latex (BWOW), mixed at 13.8 ppg with 6.48 gallons mix water per sack of cement (Fleckenstein, et al, 2000).

The thermal properties of two different system of cement that were used in the modelling are defined as following:

System A has high thermal conductivity and low heat capacity as shown in table 1

System B has low thermal conductivity and high heat capacity as shown in table 1

1

Formation fluid:

For simplification the formation fluid is assumed single phase throughout the analysis, but pressure contributions come from gas liberation (Freij-Ayoub, et al, 2007a).

Modelling sequential:

Equilibrium step:

The model is brought to equilibrium by executing an initial load step with specifying initial porosity, effective stresses, temperature and pore pressure and fixing displacements along far field boundaries.

Drilling step:

Drilling is removing the formation within the wellbore, which was under equilibrium stresses, and replacing with hydrostatic pressure of drilling mud. Therefore, removing of drilled part leads to removing the tractions on the surrounding formation equal and opposite to that exerted by the formation. The surrounding formation are deformed as typically hydrostatic pressure of drilling mud is not adequate to maintain initial equilibrium in surrounding formation. Deformation results in further stresses that jointly with far field stresses and hydrostatic pressure of drilling mud are able to reach to equilibrium (Gray, et al, 2007). To achieve the stress distribution near the wellbore after drilling as mentioned above, elements within the wellbore in the model are removed in this step.

Running the casing and cementing step:

It is assumed that casing is run and cemented immediately after drilling, therefore, in this step after adding cement and casing elements into the model, a force equal to hydrostatic pressure of the drilling mud acts on the inner surface (i.e., internal pressure) of the casing.

The interaction between cement and formation surface is modelled by defining interaction model such that formation and cement surfaces are allowed to separate (debond) but does not allow penetrate into each other (Gray, et al, 2007). To decrease the source of non-linearity in the model and obviously overcome convergence problems the cement and casing surfaces are assumed to perfectly bond, however the contact interaction in this surface can be defined if it is needed.

Cement channelling step:

The creation of the channel in the cement is modelled by removing some elements within the cement sheath in the model and filling in with formation fluid. It is assumed that the created void is filled and in communication with formation during the modelling and by changing the void geometry, its boundary conditions are not changing.

Drilling the next section step:

At this step, the wellbore temperature is increased by 10 K to simulate the heat transfer from drilling mud inside the casing. It is assumed that formation permeability is low enough that gas and water generated during gas hydrate dissociation cannot flow out of the wellbore region, resulting in an increase in the formation pore pressure.

Results and Discussions:

The pore pressure build up in the formation near the wellbore due to gas hydrate dissociation during 8 days drilling of the next section of the wellbore when there is not a void in the cement is shown in Figures 2 and 3 for cement with different thermal properties. These figures show that the pore pressure is high near the wellbore and decreases to the in-situ pore pressure in the surrounding formation. It is shown that the pore pressure calculations by ABAQUS have good agreement with the results from the thermodynamic model. In the next sections, we present the effect of formation pore pressure increasing on the stability of the casing when there is a void in the cement sheath.

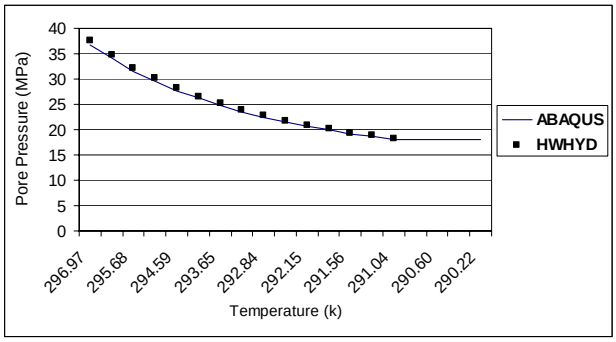

Figure 2-Pore pressure distribution from the wellbore toward the formation when when cement has thermal properties according to System A

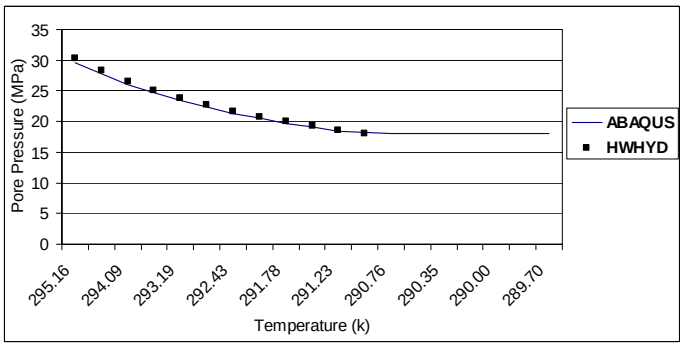

Figure 3-Pore pressure distribution from the wellbore toward the formation when cement has thermal properties according to System B

Figure 4 show the geometry of the model containing the void in the cement behind the casing. The size of void is represented by (α) as the circumferential spread of the void in the cement is measured in degrees according to what introduced by Berger, et al. (2004) and Fleckenstein, et al.(2005) .

It is assumed that there is no cement (i.e., partial cementation) at the location of the channel (void), hence the void extends from casing to the sand face. The presence of a void in the cement creates a discontinuity in the cement sheath around the casing and causes non-uniform load distribution around the total casing circumference. One part of non-uniform loads comes from the direct contact of formation fluid with outer surface of casing across the void and another part comes from the interaction of cement and the casing.

In addition, the casing is not being supported around the total circumference by the cement sheath due to the presence of void, cement discontinuity, so the casing is deformed at the void, generating high maximum Von Mises stress.

Figure 5 and 6 show the location of maximum Von Mises stress in the casing when cement has mechanical properties according to System 1 and with different thermal properties (System A and System B) but in this paper we only present the magnitude of

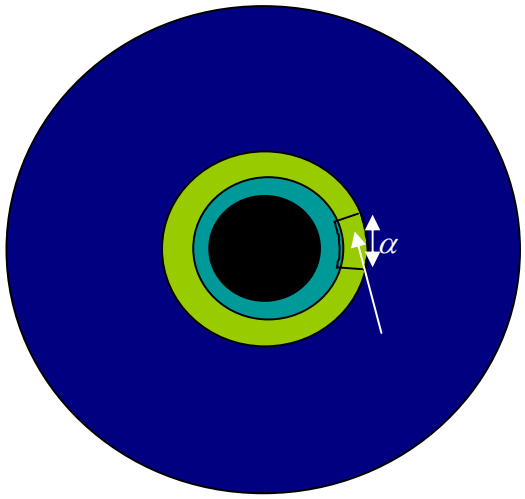

Figure 4-Geometrical shape of the model with a void (channel) in the cement sheath

maximum Von Mises stress generated due to presence of void in the Cement as listed in Table 2. In addition, we do not look at the potential of fracture initiation and propagation at the casing and cement interface.

Table 2-Maximum Von Mises stress generated in the casing after Hydrate dissociation

Void size (Degree)	Maximum Von Mises Stress (MPa)							
	System # 1				System # 2			
	System A Thermal Properties	Stress Increase (%)	System B Thermal Properties	Stress Increase (%)	System A Thermal Properties	Stress Increase (%)	System B Thermal Properties	Stress Increase (%)
Zero	154.4	0	66.69	0	166.2	0	75.99	0
9	220	42.4	74.57	11.8	303.1	82.3	91.17	19.9
18	207.9	34.6	169.9	154.7	276.4	66.3	138.5	82.2
36	237.6	53.8	337.3	405.7	283.2	70.3	316.9	317.02

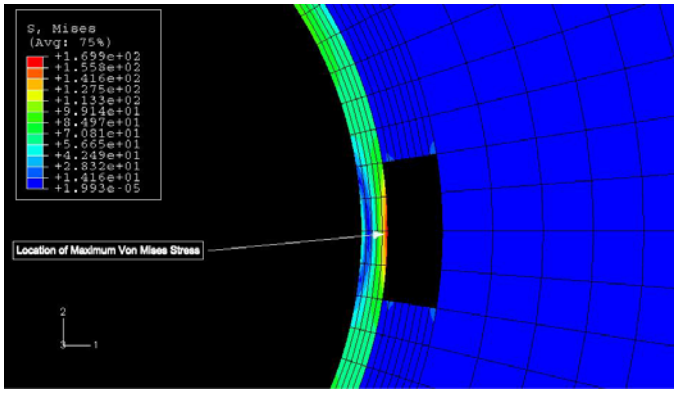

Figure 5- Maximum Von Mises stress distribution in the casing when the cement has System 1 mechanical properties and System B thermal properties

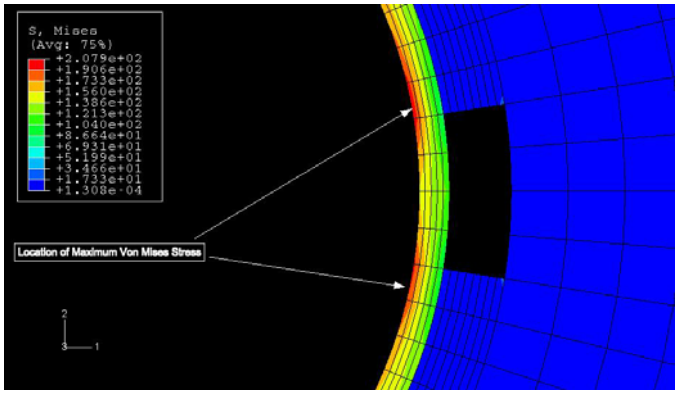

Figure 6- Maximum Von Mises stress distribution in the casing when the cement has System 1 mechanical properties and System A thermal properties

Effect of cement thermal properties on generated stress:

The cement with System B thermal properties result in the almost uniform temperature distribution behind the casing through cement and formation as shown in Figure 7. Consequently, the pore pressure generated during hydrate dissociation is almost uniform as shown in Figure 8.

In this case regardless of the cement mechanical properties, by increasing the size of the void, the maximum Von Mises stress in the casing during hydrate dissociation increases as listed in Table 2. The reason is that increasing the size of the void increases the bending stress that consequently increases the maximum Von Mises stress in the casing.

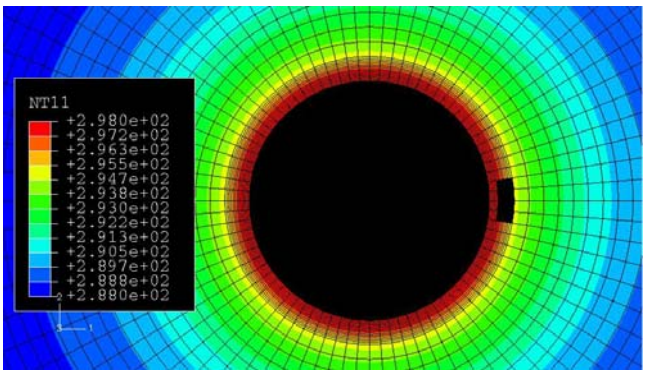

Figure 7.Temperature distribution when the cement has thermal properties according to System B

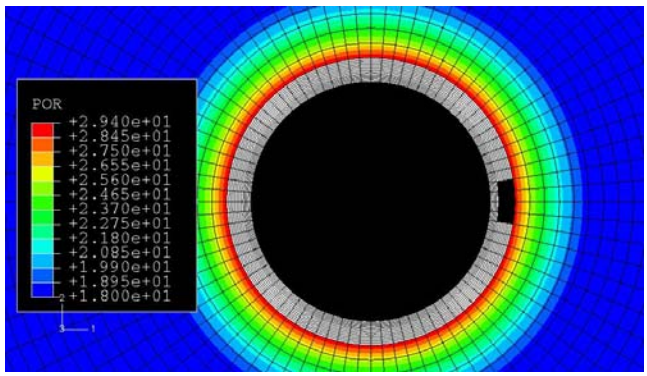

Figure 8.Pore pressure distribution when the cement has thermal properties according to System B

But the cement with System A thermal properties result in not uniform temperature distribution behind the casing through cement and formation as shown in Figure 9. Non-uniform temperature distribution generates non-uniform pore pressure distribution due to hydrate dissociation as shown in Figure 10. In this case, contrary to the previous case, increasing the size of the void does not result in a significant increase in the maximum Von Mises stress in the casing during hydrate dissociation, as shown in Table 2. The reason is that the cement has higher conductivity and lower heat capacity in comparison with the formation fluid filled the void space in the cement, so the pore pressure behind the continuous part of cement is increasing more than the discontinuous part during hydrate dissociation. This phenomenon prevents further bending (deformation) of casing and generating higher maximum Von Mises stress by increasing the size of the void in the cement sheath during gas hydrate dissociation.

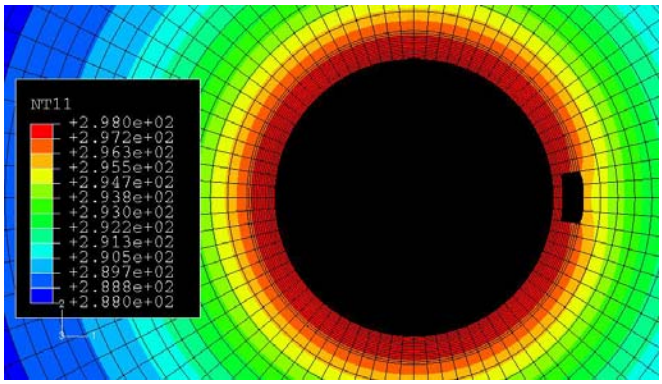

Figure 9.Temperature distribution when the cement has thermal properties according to System A

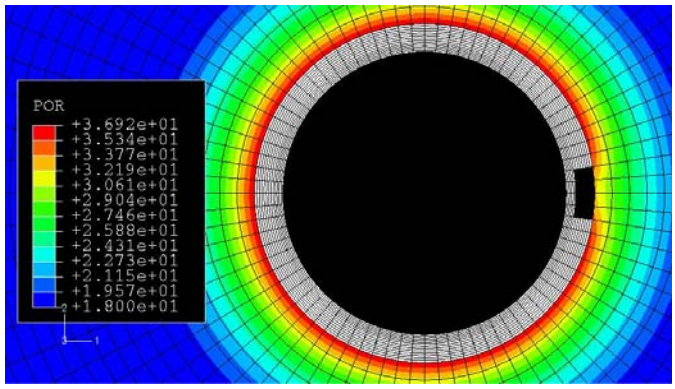

Figure 10.Pore pressure distribution when the cement has thermal properties according to System A

Effect of cement mechanical properties on generated stresses:

The modelling results show, in the cement with System B thermal properties, the System 1 mechanical properties introduces higher maximum Von Mises stress in the casing than cement with System 2 mechanical properties by increasing the size of the void (more than 9 degree) in the cement. As shown in Table 2 when the thermal properties of the cement are according to System A, an increase in void size will result in an increase in maximum Von Mises stress in cement with System 2 mechanical properties as compared to cement with System 1 mechanical properties (mechanical properties of the two systems are presented in Table 1).

Conclusions:

A numerical model that couples a well-proven thermodynamic PVT-Hydrate model (i.e., HWHYD) with ABAQUS (main features in porous medium) is developed. The model was used in investigating the effect of uniform and non-uniform loading on casing due to the presence of void (channel) in the cement sheath behind the casing in gas hydrate bearing sediments. Under the assumed boundary conditions and parameters used in the modelling, it is found that when the cement thermal properties are according to System B, regardless of cement mechanical properties the maximum Von Mises stress generated in the casing during gas hydrate dissociation in the presence of void in the cement in comparison to uniform case (no void), can increase by 317 to 405 % and this show the importance of good cement job in cements with low thermal conductivity (high heat capacity, i.e., System B). If the thermal conductivity of cement is high (low heat capacity, i.e., System A), the non-uniform pore pressure increase during gas hydrate dissociation prevents further bending (deformation) of the casing across the void, hence the maximum Von Mises stress generated in comparison to uniform case can increase to 54 to 70 %. The results of this study show that in the uniform case (no void in the cement sheath), the cement with System A thermal properties generates about 118 to 131 % higher maximum Von Mises stress than cement with System B thermal properties. This means that although the cement with System A thermal properties , in the uniform case, generates higher maximum Von Mises stress but in the presence of void, this stress does not increase significantly in comparison to the cement with System B thermal properties. However, in the cement with System B thermal properties, high void sizes (e.g., more than 18 degree) generates higher maximum Von Mises stresses than the cement with System A thermal properties. This could result in casing collapse.

It is common in drilling practices to use cement with low thermal conductivity (high heat capacity, i.e., System B) in hydrate bearing section to decrease the heat transfer through cement and consequently to decrease hydrate dissociation and pore pressure increase behind the casing. The results of this study confirm the benefits of using this kind of the cement in gas hydrate sections of the well, provided the cement job quality is good, otherwise, the stress generated in the casing during subsequent operations may lead to casing collapse.

The developed numerical model is found to be very useful in understanding the behaviour of wells drilled in gas hydrate bearing sediments. It shows the importance of good cement job during cementing of the gas hydrate section of the well. The developed model can be used as a design tool to predict the strength of casing for wells drilled in gas hydrate bearing sediments in deep offshore environment under uniform or non-uniform loading due to gas hydrate dissociation.

Acknowledgment:

This work was supported by the EPSRC (Engineering and Physical Sciences Research Council), Grant no EP/D013844/1.

Nomenclature:

C	=	new cohesion (MPa)
c_h	=	heat capacity ($JK^{-1}kg^{-1}$)
C_o	=	initial cohesion (MPa)
K	=	effective compressibility mixture of free gas, gas hydrate liquid solution (1/MPa)
$\hat{K}$	=	the permeability of the medium (mD)
k_c	=	conductivity ($Wm^{-1}K^{-1}$)
M_g	=	mass of gas (kg)
M_h	=	mass of hydrate (kg)
M_w	=	mass of water (kg)
N	=	outward normal vector
n	=	porosity
P_{ex}	=	excess pore pressure (MPa)
r_g	=	mass fraction of gas in hydrate form, 0.1292 for methane hydrate with 100% filling of the hydrate cages
S	=	surface area (m^2)
S_g	=	the volume fraction of free gas
S_h	=	the volume fraction of gas hydrate
S_r	=	saturation of wetting liquid
S_w	=	the volume fraction of water
T_e	=	the stability temperature of gas hydrate (K)
U_w	=	pore pressure (MPa)
V	=	Volume of porous media (m^3)
V_g	=	gas volume in pore space (m^3)
V_h	=	gas hydrate volume in pore space (m^3)
V_p	=	pore volume (m^3)
V_W	=	water volume in pore space (m^3)
V_w	=	seepage velocity (m/s)
ε	=	strain
ϕ	=	the piezometric head (m)
ρ	=	density of material (kg/m^3)
ρ_g	=	density of gas (kg/m^3)
ρ_h	=	density of hydrate (kg/m^3)
ρ_w	=	density of water (kg/m^3)
σ	=	stress (MPa)
$\overline{\sigma}$	=	effective stress (MPa)

$d\sigma$ = stress increment (MPa)
$d\varepsilon$ = strain increment

References:

ABAQUS User`s Manual, Version 6-7, Http://www.simulia.com/

Ahmadi, G, Ji, C, Smith, D.H, 2007, "Natural Gas Production from Hydrate Dissociation: An Axisymmetric Model", Journal of Petroleum Science and Engineering, 58, 245-258

Berger, A., Fleckenstein, W.W., Eustes, A.W., Thonhauser, G., 2004, "Effect of Eccentricity, Voids, Cement Channels, and Pore Pressure Decline on Collapse Resistance of Casing", SPE 90045, SPE Annual Technical Conference and Exhibition, Houston, Texas, 26-29 September

Birchwood, R., Noeth, S., Hooyman, P., Winters, W., 2005, "Well bore Stability Model for Marine Sediments Containing Gas Hydrates", AADE-05-NTCE-13, AADE National Technical Conference and Exhibition, Houston, Texas, April 5-7

Callister, W.D., 2007, "Material Science and Engineering, An Introduction", John Wiley & Sons

Fleckenstein, W.W., Eustes, A.W., Rodriguez, W. J., Berger, A., 2005, "Cemented Casing: The True Stress Picture", AADE-05-NTCE-14, National Technical Conference and Exhibition, Houston, Texas, April 5-7

Fleckenstein, W.W., Eustes, A.W, Miller, M.G, 2000, "Burst Induced Stresses in Cemented Well bores", SPE 62596, SPE/AAPG Western Regional Meeting Held in Long Beach, California, June 19-23

Freij-Ayoub, R., Tan, C., Clennell, B., Tohidi, B., Yang, J., 2007a, "A Well bore Stability Model for Hydrate Bearing Sediments", Journal of Petroleum Science and Engineering, 57, 209-220

Freij-Ayoub, R., Clennell, B., Tohidi, B., Yang, J., Hutcheon, R., 2007b, "Casing Integrity in Hydrate Bearing Sediments", Offshore Site Investigation and Geotechnics, London, 11-13 September

Gray, K.E., Podnos, E., Becker, E., 2007, "Finite Element Studies of Near-Well bore Region during Cementing Operations: Part-1", SPE 106998, SPE Production and Operations Symposium, Oklahoma City, 31 March-3 April

Helgerud, M.B., Dvorkin, J., Nur, A., 2000 "Rock Physics Characterization for Gas Hydrate Reservoirs Elastic Properties", Gas Hydrates Challenges for the Future, Volume 912

Kim, H.C, Bishnoi, P.R, Heidemann, R.A, Rizvi, S.S.H, 1987, "Kinetics of Methane Hydrate Decomposition", Chemical Engineering Science, Volume 42, Issue 7, Pages 1645-1653

Kimoto, S, Oka, F, Fushita, T, Fujiwaki, M, 2007, "Chemo-Thermo-Mechanically Coupled Numerical Simulation of the Subsurface Ground Deformations due to Methane Hydrate Dissociation", Computers and Geotechnics 34, 216-228

Klar, A, Soga, K, 2005, "Coupled Deformation-Flow Analysis for Methane Hydrate Production by Depressurized Wells", 3rd Biot Conference on Poromechanics, Norman, Oklahoma

Kowalsky, M., Moridis, G.J., 2007,"Comparison of Kinetic and Equilibrium Reaction Models in Simulating Gas Hydrate Behavior in Porous Media", Energy Conversion and Management, 48, 1850-1863

Moridis, G.J, 2002, "Numerical Studies of Gas Production from Methane Hydrates", SPE 75691, Gas Technology Symposium, Calgary, Alberta, 30 April-2 May

Moridis, G.J, Kowalsky, M.B, 2006, "Response of Oceanic Hydrate Bearing Sediments to Thermal Stresses", OTC 18193, Offshore Technology Conference, Houston, texas, 1-4 may

Rutqvista, J., BoÈ rgessonb, L., Chijimatsuc, M., Kobayashic, A., Jingd, L., Nguyene, T.S., Noorishada, J., Tsang, C.-F., 2001, "Thermohydromechanics of Partially Saturated Geological Media: Governing Equations and Formulation of Four Finite Element Models", International Journal of Rock Mechanics & Mining Sciences 38, 105-127

Rutqvist, J., Moridis, G.J., 2007, "Numerical Studies on the Geomechanical Stability of Hydrate-Bearing Sediments", OTC 18860, Offshore Technology Conference, Houston, Texas, 30April-3May

Smith, M.A, Kou, W, Ahmed, A, Kuzela, R, 2005, "The Significance of Gas Hydrate as a Geohazard in Gulf of Mexico Exploration and Production", OTC 17655, Offshore technology confercne, Houston, 2-5 May

Swinkels, W.J.A.M, Drenth, R.J.J, 2000, “Thermal Reservoir Simulation Model of Production from Naturally Occurring Gas Hydrate Accumulations”, SPE 68213, SPE Annual Technical Conference and Exhibition, Houston, 3-6 October

Tan, C.P., Freij-Ayoub, R., Clennell, M.B., Tohidi, B., Yang, J., 2005, “Managing Well bore Instability Risk in Gas-Hydrate-Bearing Sediments, SPE 92960, Asia Pacific Oil & Gas Conference and Exhibition, Jakarta, Indonesia, 5-7 April

Tohidi, B., A. Danesh and A. C. Todd (1995). "Modelling Single and Mixed Electrolyte-Solutions and Its Applications to Gas Hydrates." Chemical Engineering Research & Design 73(A4): 464-472.

Xu, W., 2006, “Excess Pore Pressure Resulting from Methane Hydrate Dissociation in Marine Sediments: A Theoretical Approach”, Journal of Geophysical Research, Vol 111

Yousif, M.H, Li, P.M, Selim, MS, Sloan, E.D., 1990, “Depressurization of Natural Gas Hydrates in Berea Sandstone Cores”, J.Inclusion Phenom, Mol.Recognit.Chem.8, 71-88

Yousif, M.H, Abbas, H.M, Selim, M.S., Sloan, E.D, 1991, “Experimental and Theoretical Investigation of Methane-Gas-Hydrate Dissociation in Porous Media”, SPE Reservoir Eng.69-76, February